Polymer Bulletin
https://doi.org/10.1007/s00289-024-05311-z

ORIGINAL PAPER

Physicochemical characteristics and oil sorption behaviours of novel polymeric materials based on modifications of water hyacinth (*Eichhornia crassipes*) fibres

Nguyen Thanh Tung[1] · Ninh The Son[1] · Pham Thi Thu Ha[1] · Nguyen Thi Mien[1] · Le Thi Mai[2] · Nguyen Duc Duy[2] · Pham Ngoc Anh[2] · Nguyen Ngoc Linh[3] · Nguyen Trung Duc[1]

Received: 28 November 2023 / Revised: 28 March 2024 / Accepted: 7 May 2024

Abstract

The aim of the current study is to modify water hyacinth fibre (WHF), which are then used to produce novel oil sorption polymers. Two synthetic materials were derived from acetylation by acetic anhydride using *N*-bromosuccinimide (NBS) as a catalyst and the graft co-polymerisation of butyl acrylate (BA) using 2,2′-azobisisobutyronitrile (AIBN) as an initiator. Physicochemical properties were comprehensively characterised by Fourier transform infrared spectroscopy, scanning electron microscopy, X-ray diffraction, contact angle, and thermogravimetric analysis. In the seawater/crude oil system, the best oil sorption capacity values of the raw WHFs and their acetylated-WHF and graft co-polymer WHF-g-BA were 7.46 g/g, 20.16 g/g, and 25.47 g/g, respectively. The sorption kinetic and isotherm studies exhibited that the oil sorption of the co-polymer WHF-g-BA is ruled by pseudo-second-order kinetic and Freundlich isotherm models. The reusability of the WHFs and their synthetic materials has reached 6 cycles of sorption/desorption, and this property of the co-polymer is always better than that of acetylated and original fibres.

Keywords Water hyacinth fibre · Cellulose · Oil sorbent · Acetylation · Graft co-polymerisation

✉ Nguyen Trung Duc
ducnt224@gmail.com

[1] Institute of Chemistry, Vietnam Academy of Science and Technology, 18 Hoang Quoc Viet, Cau Giay, Hanoi 10000, Vietnam

[2] Lac Trung Technology and Trading Services Company Limited, 350 Lac Trung, Hai Ba Trung, Hanoi 10000, Vietnam

[3] Thanh Do University, Kim Chung, Hoai Duc, Hanoi City 10000, Vietnam

Published online: 21 May 2024

Introduction

One of the most important sources of energy is crude oil. It has been used as the primary material for transportation vehicles for a very long period. The oil demands have increased in the industrial world. The spillage of oils, which happens during production, transportation, and storage, immediately affects aquatic life, the local economy, tourism, and leisure activities. Oil sorbents can be categorised as either synthetic or natural materials, and most are made of synthetic materials. However, they are very pricey and non-biodegradable. Hence, the search for oil sorbents from natural sources is warranted [1].

The most prevalent renewable organic substance in nature is cellulose. It is a raw biomass material that is simple to obtain. It can be found in large quantities in plants like wood, bamboo, cotton, and hemp. In addition, some marine species, such as algae, and even bacteria, have a small proportion of cellulose [2]. They are also easily interwoven into network structures, which have a high specific surface area, and are thermally stable and renewable [2, 3]. In addition, cellulose fibres and their modified forms were considered promising adsorbents for the surface separation of petroleum pollutants with good absorption capabilities in recent years. Oil spill cleanup in actual marine environments remains challenging despite the development of numerous filter-type materials having separation emulsion capabilities for oil–water isolation. The viscous crude oils can clog filter pores and quickly contaminate filter materials, but gravity-driven or pressure-driven filtration procedures need to pre-collect the oil–water mixture before filtering. As a result, adsorption-type oil–water separation materials have lately become a hot research topic [3].

Water hyacinth (WH) is a rhizomatous plant with long pendant adventitious roots. It floats freely on the water's surface and is abundant in tropical regions like Vietnam. Due to its rapid growth (125 tons/1 surface ha/6 months) [4], WH poses major risks to human health and the environment in the water ecosystem and water transportation network. It is also a breeding ground for insects that spread disease. There have been several attempts to use WH for handicraft goods, fertilisers, and biofuels [5], but these efforts have been hampered by low product conversion rates and the high cost of pretreatment. However, WH can serve as a feedstock for aerogel because it contains a large amount of cellulose (up to 50% by weight) [6]. Additionally, WH is very porous and contains a great deal of water; as a result, it can be broken into little pieces during the pretreatment step without drying out, which lowers the energy needed for the synthesis process [6].

Chemical modifications of raw cellulosic fibres by immersion in chemical solutions (alkali, peroxides, silane, etc.) tend to remove weak components such as hemicelluloses and lignin, thereby improving the fibres' mechanical and adsorption capabilities [7]. To date, a few studies were carried out to create new composites by the treatment of water hyacinth fibres (WHFs) with alkali or silane [8, 9]. In the current study, WHF modifications by the acetylation process and butyl acrylate grafting to produce two novel oil sorption materials are performed. Oil sorption behaviours of the novel synthetic materials are compared with the original WHFs. Sorption kinetics, isotherm models, and reusability are also considered.

Materials and experiments

Materials

The fresh WH (water hyacinth) stems were gathered from Nghean, Vietnam, in 08/2022. All chemicals, including butyl acrylate (BA), 2,2′-azobisisobutyronitrile (AIBN), *N*-bromosuccinimide (NBS), *N*, *N*-dimethyl formamide (DMF), NaClO, acetic anhydride, acetone, toluene, and absolute ethanol (EtOH), were supplied by Sigma-Aldrich.

Cellulosic extraction

The fresh WH stems were crushed into 1–2-mm sized particles and dried at 105 °C for 2 h before being extracted with an ethanol-toluene mixture for 3.5 h at 100 °C [10]. To produce the purified fibres, 500 mL of a NaClO solution (3%) was used to bleach the brown fibres that still included impurities. This process was heated over a water bath at 80 °C for 2 h. To eliminate the surplus acids, ethanol was used after multiple rounds of distilled water washing on the resulting celluloses. The washing procedure was continued until the cellulose's colour turned completely white.

Synthesis

Acetylation of the WHFs

Acetylation of the WHFs with acetic anhydride was carried out under a nitrogen environment in a 250-mL three-neck flask coupled with a condenser [11, 12]. The WHFs and acetic anhydride at different ratios (1:1, 1:5, 1:10, and 1:15, w/v) were incorporated into the flask. The flask was then placed in an oil bath and set at the required temperature (70–100 °C) for 30–150 min. The NBS initiator (1.0–2.5 mol/L) was slowly added to the reaction mixture and stirred. At the end of the reaction, the acetylated-WHF product was washed and extracted by a Soxhlet apparatus with acetone for 6 h. Finally, it was dried under vacuum at 60 °C to constant weight.

The weight percent gain (WPG) was expressed as follows:

$$\mathrm{WPG}\,(\%) = (A_2 - A_1)/A_1 \times 100\% \tag{1}$$

where WPG stands for an increase in the dry weight of WHFs after acetylation. A_2 and A_1 denote acetylated and unacetylated WHFs, respectively.

Graft polymerisation

Graft polymerisation of the WHFs was carried out as described previously [13–15]. The reaction was performed under a nitrogen environment in a 250-mL three-neck flask coupled with a condenser. The WHFs (0.6 g) were soaked and stirred in DMF (15 mL). The BA monomer (0.5–2.0 mol/L) was then added, and the reaction

temperature was regulated from 65 to 80 °C. The AIBN initiator (0.04–0.1 mol/L) was then incorporated. After the appropriate reaction time (60–210 min), the graft product WHF-g-BA was incorporated into 220 mL of the absolute EtOH for precipitation. The obtained co-polymer continued to be washed with EtOH (60 mL × 3 times) and extracted with acetone (60 mL × 3 times) to discard the homopolymer of BA. In the last step, the WHF-g-BA was then chopped into small pieces and dried under vacuum at 50 °C to a constant weight.

The GY (graft yield) was calculated as follows:

$$\mathrm{GY}\,(\%) = (B_2 - B_1)/B_1 \times 100\% \tag{2}$$

where B_2 and B_1 represent the weights of WHF-g-BA and BA, respectively.

Oil sorption

The pre-calculated amounts of the crude oil and seawater were introduced to a 1.5-L glass container in the thermostatic shaker water bath at operating conditions of 40 °C and 100 rpm [16]. Each tested sample (WHFs, acetylated-WHF, and WHF-g-BA) was then steeped into this system for 20 min, which was continuously separated and drained for 8 min and re-weighed. Water sorbed with oil has been measured by drying the wet (oil and water) fibres at 105 °C for one day. The calculation of water (W_C) and oil (O_C) sorption contents were displayed as follows:

$$W_C = M_{(W+O)} - M_{D(O)} \tag{3}$$

$$O_C = M_{D(O)} - M_F \tag{4}$$

where $M_{(w+o)}$, $M_{D(O),}$ and M_F stand for the weights (g) of wet (oil and water) sample, dried wet (oil) sample, and initial sample, respectively.

The OS (oil sorption, %) from the oil/water system was expressed as follows:

$$\mathrm{OS}\,(\%) = \left[\left(M_{D(O)} - M_F\right)/M_F\right] \times 100 \tag{5}$$

The OSC (oil sorption capacity), referred to as g of oil/g of sample, can be calculated as follows:

$$\mathrm{OCS} = O_C/M_F = (M_{D(O)} - M_F)/M_F \tag{6}$$

The physicochemical properties and microstructure evaluations

The LactoScope 300 FTIR spectrometer at a wavelength range of 4000–400 cm^{-1} was used to measure the IR spectrum. Using the JEOL 6390 model SEM, the surface morphology of the tested samples was investigated. The Model D5000 Siemens diffractometer was used to obtain the X-ray diffraction data with scanning between 5° and 50°. The TGA data were collected from a Labsys TG-DSC 1600 (heating rate 10°/min from 25 to 800 °C). In addition, both hydrophobic and hydrophilic

properties were considered using OCA50 contact angle instruments using water and oil droplets.

Results and discussion

Effects of different parameters on WHF acetylation

From Table 1, it can be seen that the WPG increases with increasing time. The highest WPG value of 30.05% is found at 120 min. However, the WPG value has been observed to gradually decrease beyond 120 min. As can be seen, the longer the reaction period is, the more product is produced, and less acetic anhydride is present, resulting in higher values [11, 12]. Considering the temperature effect, the maximum WPG value of 30.05% was associated with 90 °C. The increase in temperature from 70 to 90 °C causes cleavages of hydrogen bonds, strengthening the cellulosic fibres. This also enhances acetic anhydride diffusion into the fibres [11, 12]. Additionally, increasing the temperature accelerates the reaction speed and collision of the nuclei participating in the reaction, which promotes the reaction rate. However, cellulosic acetylation is a reversible process that produces acetic acid as a by-product. While

Table 1 Effect of different parameters on acetylation of the WHFs (water hyacinth fibres)

Time (min)	Temp. (°C)	Fibres/acetic anhydride ratio	Initiator (mol/L)	WPG (%)
Effect of time				
30	90	1:10	2	14.52
60	90	1:10	2	25.46
90	90	1:10	2	28.45
120	90	1:10	2	30.05
150	90	1:10	2	29.12
Effect of temperature				
120	**70**	1:10	2	15.26
120	**80**	1:10	2	24.56
120	**90**	1:10	2	30.05
120	**100**	1:10	2	25.42
Effect of rate of the WHFs/acetic anhydride				
120	90	**1:1**	2	16.25
120	90	**1:5**	2	27.15
120	90	**1:10**	2	30.05
120	90	**1:15**	2	26.24
Effect of initiator concentration				
120	90	1:10	**1.0**	18.46
120	90	1:10	**1.5**	24.25
120	90	1:10	**2.0**	30.05
120	90	1:10	**2.5**	16.68

Bold values indicate the conditions were changed

the temperature continues to increase beyond 90 °C, the reaction to create a by-product will easily happen, thereby decreasing the WPG value [11, 12].

The rate of the WHFs/acetic anhydride is the third factor that greatly affected the acetylated yield. As shown in Table 1, the lowest WPG value of 16.25% was accomplished by the ratio of 1:1 w/v. The highest WPG value of 30.05% was in parallel with the ratio of 1:10, but a higher amount of acetic anhydride is not favourable (WPG of 26.24% at the ratio of 1:15). It was demonstrated that an increase in the concentration of acetic anhydride results in an increase in contact surface between acetic anhydride and cellulose, accelerating the reaction speed and raising the WPG [11, 12]. However, if the concentration continues to increase, the WPG value tends to decrease with acetic acid being a by-product. Hence, the optimal ratio for the WHF acetylation is 1:10. In the last case, the lowest WPG value of 16.25% was associated with the NBS initiator concentration of 1.0 mol/L, whereas the WPG achieved the highest percentage by using 2.0 mol/L of NBS. After this range, the WPG value has been drastically reduced (Table 1). It is hypothesised that NBS is a good source for creating the Br^+ cation, activating the carbonyl group of acetic anhydride to create a highly acylated centre CH_3–CO–N–($OCCH_2CH_2CO$–) (Fig. 1). After that, this agent reacted with the WHF–OH, resulting in the production of the WHF–O–CO–CH_3 [17, 18].

Effects of different parameters on the WHF grafting

With increasing reaction time the GY value increased from 25.17 to 46.60% within the first 3 h (Table 2). Nonetheless, no discernible variation in the graft add-on was observed between 3 and 4 h of reaction times. Therefore, the ideal time for grafting was determined to be 3 h, because sufficient time was provided to promote the copolymerisation reaction in the first stage, which led to the swelling of WHF particles and the diffusions of initiator and monomer, as well as the minimal homopolymerisation process of monomers [14]. However, the radical quenching brought on by extended heat treatment and the predominance of homopolymeric reactions among monomers can be blamed for the unstable GY after 3 h [14].

The GY is also dependent on the temperature change, as evidenced when the temperature was increased from 65 to 75 °C, the GY correspondingly increased from 30.1 to 42.6%. At a temperature higher than 75 °C, the GY value was found to be reduced, e.g. the GY value achieved 35.3% at 80 °C. The increased extent of monomer mobility and diffusion from the aqueous bulk phase to the cellulose phase, as well as the faster rate of initiator dissociation, could be the cause of the larger GY with an increase in temperature [13]. However, the GY tends to diminish beyond 75 °C, which is most likely caused by a creation of unstable complexes by the initiator, along with the predominance of the termination processes [13, 14].

In the next observation, the GY was found to be remarkably increased with an increase in the BA monomeric concentration from 0.5 mol/L to 1.5 mol/L. This phenomenon can be deduced from the availability of monomer for grafting in the early stage. However, at higher monomeric concentration (beyond 1.5 mol/L), the homopolymer processes may be superior to grafting, causing only a slight increase

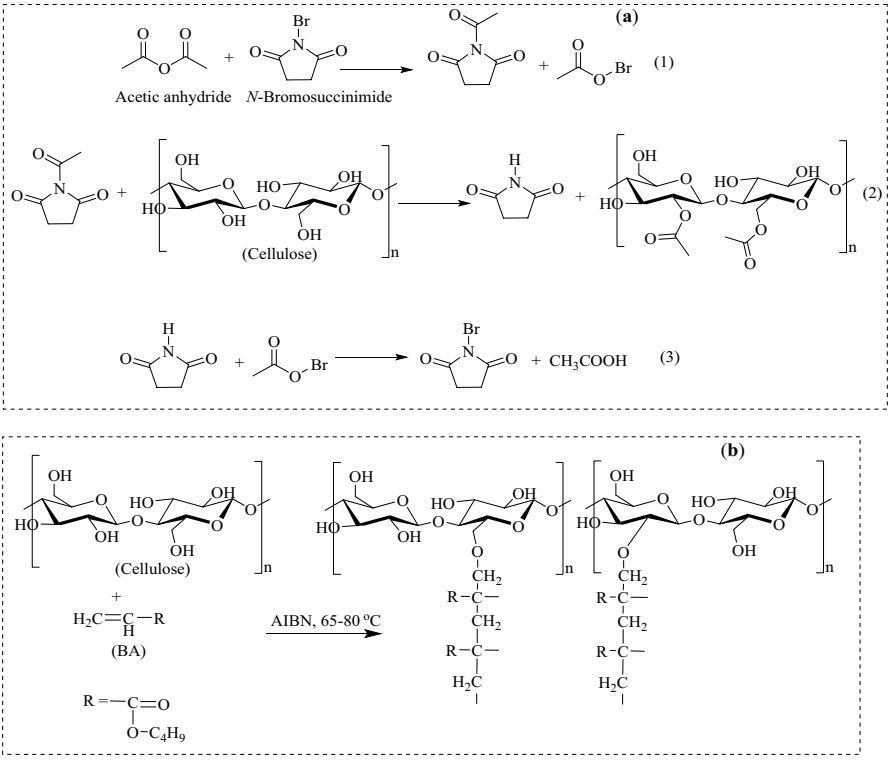

Fig. 1 Mechanisms of the acetylation (**a**) and graft (**b**) with the representative OH groups of the WHFs

in the yield of the graft [13–15]. Therefore, BA at a concentration of 1.5 mol/L can be considered as the optimal concentration for the WHF grafting. Lastly, the GY values of 24.5, 35.7, 42.6, and 22.2% correspond to the AIBN consumable amounts of 0.04, 0.06, 0.08, and 0.1 mol/L, respectively. It has been demonstrated that the AIBN initiator, at a concentration of 0.04–0.08 mol/L, plays a significant role in the generation of free hydroxyl radicals in the cellulosic network and methylene radicals in the poly(BA). Nevertheless, because the homopolymeric reactions among the BA monomers caused an increase in the viscosity of the reaction system, raising the initiator AIBN concentration above 0.08 mol/L lowered the graft process [13].

FTIR analysis

From Fig. 2, it can be seen that the acetylated fibres and grafted copolymer induced significant differences in the IR spectral data, compared to that of the raw material. The –OH stretching vibrations of the cellulosic fibres in all three materials are responsible for the intense broad peak absorption above 3330 cm^{-1}, whereas the CH stretching vibrations of the CH_3 and CH_2 groups can be attributed to the peaks at about 2900 cm^{-1} [19, 20]. The broad peaks at 1030.24, 1030.67, and 1029.59 cm^{-1}

Table 2 Effect of different parameters on grafting of the WHFs

Time (min)	Temp. (°C)	Monomer (mol/L)	Initiator (mol/L)	GY (%)
Effect of time				
60	75	1.5	0.08	25.17
90	75	1.5	0.08	30.24
120	75	1.5	0.08	32.16
150	75	1.5	0.08	37.45
180	75	1.5	0.08	42.60
210	75	1.5	0.08	42.58
Effect of temperature				
180	**65**	1.5	0.08	30.08
180	**70**	1.5	0.08	34.23
180	**75**	1.5	0.08	42.60
180	**80**	1.5	0.08	35.26
Effect of monomer concentration				
180	75	**0.5**	0.08	26.18
180	75	**1.0**	0.08	38.45
180	75	**1.5**	0.08	42.60
180	75	**2.0**	0.08	28.46
Effect of initiator concentration				
180	75	1.5	**0.04**	24.46
180	75	1.5	**0.06**	35.67
180	75	1.5	**0.08**	42.60
180	75	1.5	**0.1**	22.15

Bold values indicate the conditions were changed

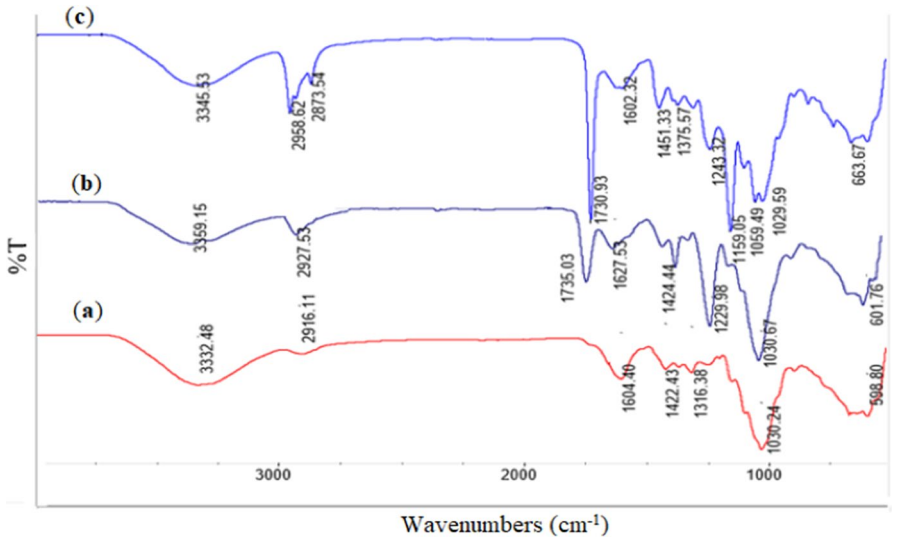

Fig. 2 The IR spectra of the WHFs (**a**), acetylated-WHF (**b**), and WHF-g-BA (**c**)

in the IR spectral data of WHFs, acetylated-WHF, and WHF-g-BA, respectively, have been nominated for C–O valence vibrations [20]. Significantly, the new sharp peaks at 1735.03 and 1730.93 in the corresponding IR spectral data of acetylated-WHF and WHF-g-BA are due to carbonyl stretching vibrations, which otherwise are absent in the raw WHFs, indicating strong evidence of successful hydrophobic modifications.

SEM analysis

The surface morphology of the WHFs, acetylated-WHF, and WHF-*g*-BA is shown in Fig. 3. The raw material has a rough surface, uneven, with a notched structure. After grafting, the acetylated-WHF has been structurally formed with porous layers. This causes cellulose to be successfully dissolved in acetic anhydride during the acetylation process. Because of the formation of voids in the fibre structure brought on by the shorter acetylation period and the accompanying variation in acetyl concentration, the final product has a different morphology from the original cellulose. Regarding the WHF-g-BA, it has an even and regular surface that is covered with poly(BA). The BA monomer is firmly attached to the original cellulose fibres by chemical bonding [21, 22].

TGA analysis

The TGA curves of the WHFs, acetylated-WHF sample, and WH-g-BA are shown in Fig. 4. With differences in their chemical structures, they correspondingly decompose at different temperatures. In the TGA diagram of the WHFs, dehydration occurred at a temperature of less than 300 °C, while a peak of 399.87 °C can be assigned to the cellulosic decomposition. For the initial stage of the TGA of the acetylated-WHF sample, the weight loss of 7.67% at 104.49 °C was due to dehydration. Beyond this temperature, the drastic cellulosic decomposition of the sample resulted in significant weight loss, which was 62.53% at 324.02 °C. In the TGA profile of the WH-g-BA sample, three peaks at 104.49 °C, 324.02 °C, and 460.83 °C were derived from the dehydration, cellulosic chain destruction, and poly(BA) graft decomposition [23, 24].

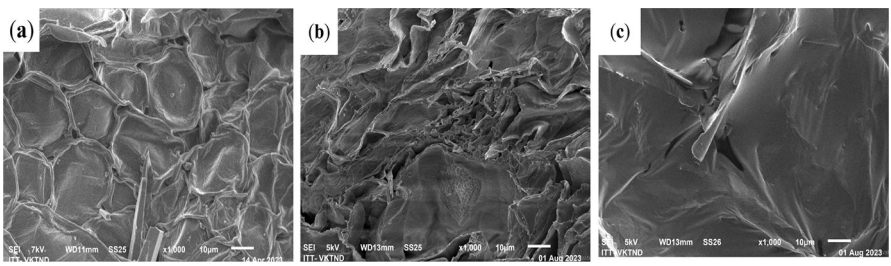

Fig. 3 The SEM images of the WHFs (**a**), acetylated-WHF (**b**), and WHF-g-BA (**c**)

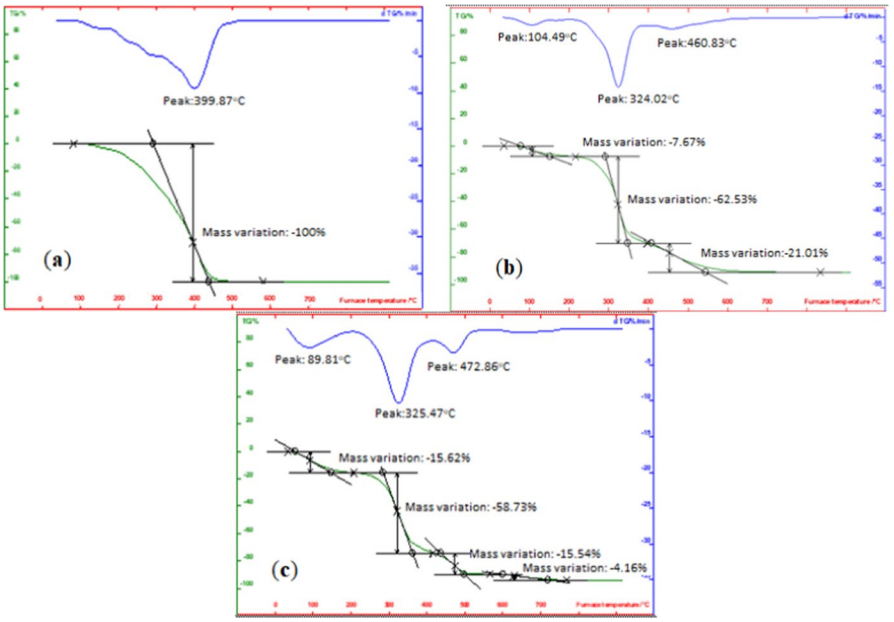

Fig. 4 The TGA curves of the WHFs (**a**), acetylated-WHF (**b**), and WHF-g-BA (**c**)

Contact angle analysis

It is important to comprehend the wetting and adhesion of absorbent products used in oil spill cleanup [25]. The hydrophobic/hydrophilic and oleophilic characters of the three studied samples are shown in Fig. 5 and Table 3 and were obtained by using the water and crude oil droplets method, based on wettability measurements [25]. In comparison with the natural WHFs, which recorded an angle of 52.3° in

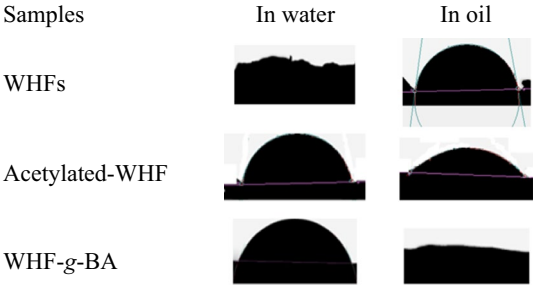

Fig. 5 Contact angles of the WHFs, acetylated-WHF, and WHF-g-BA

Table 3 Contact angles of the studied materials in the water and oil

Samples	Water	Oil
WHFs	52.3°	63.4°
Acetylated-WHF	65.9°	25.8°
WHF-g-BA	80.5°	15.8°

water, the hydrophilic property of its two synthetic materials was found to be down-regulated at 65.9° and 80.5°, respectively. The obtained results also indicated that the oleophilic character of the raw WH fibre (63.4°) was enhanced and recorded at 25.8° and 15.0° in the cases of the acetylated-WHFs and WHF-g-BA, respectively. Obviously, the acetyl and monomer butyl acrylate groups in the oil-absorbing materials are hydrophobic and oleophilic, which could explain these results.

XRD analysis

The XRD image has been employed to evaluate the crystalline nature of the materials. The XRD patterns of WHFs, acetylated-WHF, and WHF-g-BA are outlined in Fig. 6. For the original WHFs, a sharp peak with a high intensity of 720.5 a.u. at the 2θ angle of 22° revealed the crystalline nature of the material. At the same 2θ angle of 22°, the XRD images of acetylated-WHF and WHF-g-BA have been accompanied by intensities of 265.43 a.u. and 98.22 a.u., respectively. This reduction in the crystallinity is due to the presence of cellulosic acetate and co-polymer graft. It can be noted that acetylation and branching co-polymerisation with poly(BA) onto the cellulosic framework cause a decrease in the crystallinity of the cellulose fibres [26, 27].

Effects of the hydrophobic modification methods

The effects of the modification technique on the OSC have been considered in the seawater, oil, and oil/seawater systems under operating conditions (Table 4 and Figs. 7, 8, 9).

In the seawater sorption assessment: The water hydrophobicity of the graft co-polymer was better than that of both the acetylated and raw fibres (Table 4 and Fig. 7). The optimal OCS values were 15.23 g/g, 2.05 g/g, and 1.46 g/g for the WHFs, acetylated-WHF, and WHF-g-BA, respectively, at 10 min. It turns out that

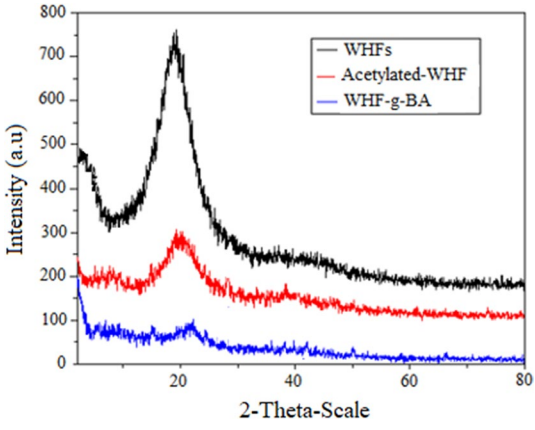

Fig. 6 The XRD curves of the WHFs, acetylated-WHF, and WHF-g-BA

Table 4 Effect of modification technique on the OSC (oil sorption capacity)

Samples	Models	The optimal operating condition	OSC (g/g)
WHFs	SW-SA	WHF (0.1 g), seawater (1.0 L), 40 °C, 10 min, and 100 rpm	15.23
	O-SA	WHF (0.1 g), oil (1.0 L), 40 °C, 10 min, and 100 rpm	9.52
	O/SW-SA	WHF (0.1 g), seawater (1.0 L), oil (40 mL), 40 °C, 10 min, and 100 rpm	7.46
Acetylated-WHF	SW-SA	Acetylated-WHF (0.1 g), seawater (1.0 L), 40 °C, 10 min, and 100 rpm	2.05
	O-SA	Acetylated-WHF (0.1 g), oil (1.0 L), 40 °C, 10 min, and 100 rpm	22.65
	O/SW-SA	Acetylated-WHF (0.1 g), seawater (1.0 L), oil (40 mL), 40 °C, 10 min, and 100 rpm	20.16
WHF-g-BA	SW-SA	WHF-g-BA (0.1 g), seawater (1.0 L), 40 °C, 10 min, and 100 rpm	1.46
	O-SA	WHF-g-BA (0.1 g), oil (1.0 L), 40 °C, 10 min, and 100 rpm	28.65
	O/SW-SA	WHF-g-BA (2.0 g), seawater (1.0 L), oil (40 mL), 40 °C, 10 min, and 100 rpm	25.47

SW-SA, seawater sorption assessment; O-SA, oil sorption assessment; O/SW-SA, oil/seawater sorption assessment

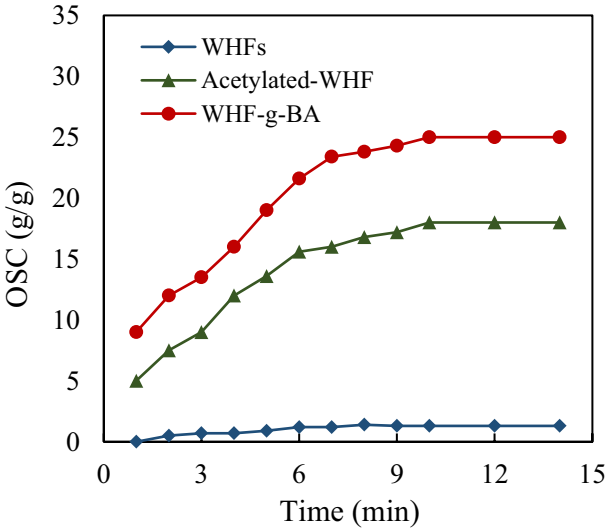

Fig. 7 Sorption assessment of the WHFs, acetylated-WHF, and WHF-g-BA in the seawater

Fig. 8 Sorption assessment of the WHFs, acetylated-WHF, and WHF-g-BA in the oil

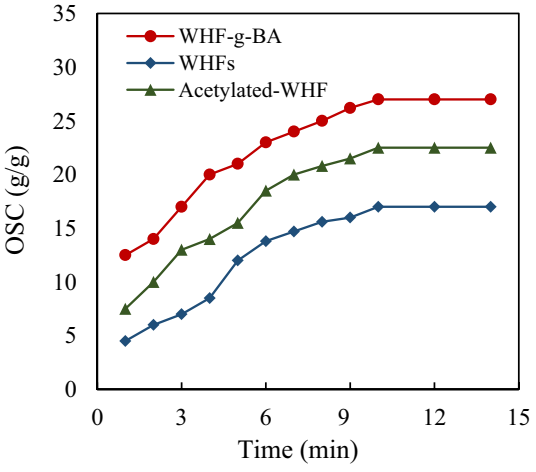

the process of acetylation and co-polymerisation of the WHFs induced a protective layer to the sorption of water, which resulted in the hydrophobic features [28, 29].

In the oil sorption assessment: The optimal OCS values were recorded to be 9.52 g/g, 22.65 g/g, and 28.65 g/g for the WHFs, acetylated-WHF, and WHF-g-BA, respectively, at 10 min (Table 4 and Fig. 8). Herein, the porous hydrophobic surface of the acetylated-WHF acted as sorbed sites [30]. For the graft co-polymerisation, the hydrophobic poly(BA)-grafted branches were distributed on the surface of the WHF. As a consequence, the obtained material became hydrophobic and oleophilic.

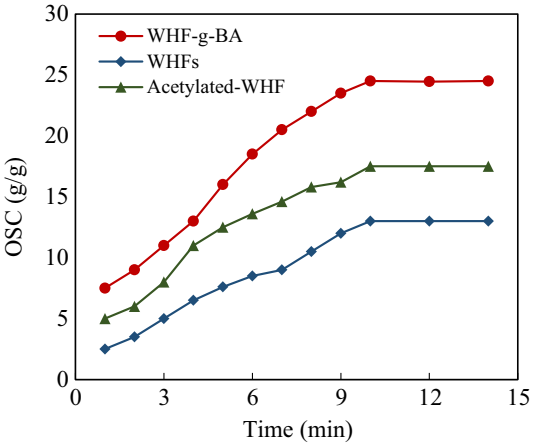

Fig. 9 Sorption assessment of the WHFs, acetylated-WHF, and WHF-g-BA in the oil/seawater system

In the oil/seawater sorption assessment: Similar results to oil sorption were obtained since the optimal OCS of the WHF-g-BA (25.47 g/g) has been always better than that of the acetylated-WHF (22.65 g/g) and the WHFs (7.46 g/g) (Table 4 and Fig. 9). Treatment of the WHFs with acetic anhydride increased the hydrophobic property because of the ester reaction between hydroxyl groups of the fibre and acetyl groups of acetic anhydride, which caused the fibre to be coated with a hydrophobic film, leading to the packaging of fibre with a water-repellent layer that reduced the water sorption. The results further demonstrated that the graft co-polymer was more uniformly distributed on the surface of the WHFs, and the material evolved into a homogenous spatial lattice polymer with a porous structure. This allowed the obtained material to have certain solvents held inside its structure [31]. Significantly, the OCS value of WHF-g-BA in the current study is much better than that of rice straw-g-BA (20.56 g/g), sawdust-g-BA (20.52 g/g), and *Luffa* fibre-g-BA (20.60 g/g) [13–15]. In another study, modification of flax fibres by acetylation and microwave methods resulted in OSC values of 24.54 and 17.42 g/g, respectively [16].

Sorption dynamics

The effects of the WHF modifications in three mediums indicated that the co-polymer WHF-g-BA has the highest oil sorption and lowest water sorption, followed by the acetylated material, and then raw fibre. In this scenario, the study shifts to the dynamic evaluations for the potential co-polymer.

Effect of contact time

The effect of sorption time was determined in a range of 1–20 min by adding the co-polymer (0.1–0.5 g) and crude oil (10–35 mL) in a 1.0-L seawater glass container at the operating conditions of 30–50 °C and 100 rpm. The obtained results (Table 5)

Table 5 Dynamic parameters of oil sorption in seawater by WHF-g-BA

The operating conditions		OS (%)	OSC (g/g)
Time: (25 mL, 0.1 g, 100 rpm, 40 °C)	2 min	66.27	3.56
	4 min	77.18	8.56
	6 min	92.45	12.23
	8 min	95.56	18.45
	10 min	99.96	25.47
	12 min	99.95	25.47
	14 min	99.95	25.47
	16 min	99.94	25.46
	18 min	99.96	25.46
	20 min	99.95	25.46
Sorbent dose (g): (25 mL, 10 min, 100 rpm, 40 °C)	0.1 g	99.95	25.47
	0.2 g	99.95	20.56
	0.3 g	99.94	13.25
	0.4 g	99.94	12.48
	0.5 g	62.46	12.05
Initial oil concentration (g/L): (0.1 g, 10 min, 100 rpm, 40 °C)	10 mL/L	99.96	10.17
	15 mL/L	99.96	15.27
	20 mL/L	99.96	20.34
	25 mL/L	99.96	25.47
	30 mL/L	82.57	25.43
	35 mL/L	71.12	25.27
Temperature: (25 mL, 10 min, 0.1 g, 100 rpm)	30 °C	72.86	23.05
	35 °C	89.67	24.28
	40 °C	99.95	25.47
	45 °C	89.45	24.58
	50 °C	72.75	23.45

revealed that the OSC value increased with time and reached the highest value of 25.47 g/g at 10 min. After this period, it remained stable. This demonstrated that the oleophilic contact and surface capillary force, which increased the amount of sorbed oil onto the fibre's surface, caused the oil sorption mechanism to occur rapidly during the early stages of oil sorption. Van der Waals forces can then cause the oil to be absorbed into interior fibre pores. However, because the fibres' sorption active sites are fully utilised, the oil removal will gradually increase until it reaches the equilibrium condition [32].

Effect of sorption dosage

As shown in Table 5, the use of the co-polymer increased from 0.1 g to 0.5 g, and the oil sorption decreased from 99.95 to 62.46%, respectively. Notably, the OCS value was reduced from 25.47 to 12.05 g/g. As a result of sorption sites aggregating,

a higher dose of fibre causes a decrease in sorption capacity. Thus, the amount of sorbed oil on a unit mass of absorbent material decreased as the fibre dose rose, which was followed by a decrease in the oil sorption capacity [33].

Effect of initial oil concentration

The crude oil in a range of 10–35 mL in 1.0 L seawater was used to study the effect of initial oil concentration on the OS and OSC values at a constant condition of 0.1 g sorbent dose, 40 °C, 10 min, and 100 rpm. From Table 5, the OS value noticeably declined from 99.96 to 71.12% for varying initial oil feed from 10 to 35 mL/L. The OCS has risen from the lowest value of 10.17 g/g (at 10 mL/L) to the maximal value of 25.47 g/g (at 25 mL/L). After this range, the OSC was gently declined. The reduction in the oil sorption percentage is caused by the fibres' capacity to store oil in their pores, which decreases the number of sorption sites by increasing the amount of oil fed into the fibres [34].

Effect of temperature

Temperature is a crucial factor in the sorption of crude oil from seawater due to changes in the oil viscosity. Table 5 shows that the OSC increased from 23.05 to 25.47 g/g with increasing temperature from 30 to 40 °C. This increase can be explained by a decrease in the oil viscosity since more energy is required to bind oil molecules to the sorbent surface. After 40 °C, the bonds among oil molecules are weakened and the oil sorption process becomes unpredictable, which lowers the OCS values possibly meaning that because of its exothermic nature, the sorption process works best at lower temperatures. It also takes into account the fact that the oil molecules diffuse more quickly and require less time to absorb. The great propensity of oil molecules to migrate from the sorbent's surface to the bulk phase, on the other hand, causes the boundary layer thickness to decrease at higher temperatures, which significantly lowers the sorption trend. In addition, the oil molecule's overall energy is raised, enhancing its ability to escape [35].

Sorption kinetics

To estimate the sorption kinetics of oil uptake from the oil/seawater system, the pseudo-first-order, pseudo-second-order, and Elovich kinetic models are appropriate [36]. The agreement of sorption models with experimental results was evaluated by the X^2 (Chi-square analysis) and R^2 (correlation coefficient).

$$\text{Pseudo-first-order model:} \quad \mathrm{d}q_t/\mathrm{d}_t = K_1(q_\mathrm{e} - q_t) \tag{7}$$

$$\text{Pseudo-second-order model:} \quad \mathrm{d}q_t/\mathrm{d}_t = \mathrm{K}_2\left(\mathrm{q}_\mathrm{e} - q_\mathrm{t}\right)^2 \tag{8}$$

Table 6 The sorption kinetics of the WHF-g-BA at 25 mL oil/1.0 L seawater system, 100 rpm, and 40 °C

Pseudo-first-order	Experiment	Pseudo-second-order	Experiment	Elovich	Experiment
q_e (g/g)	38.342	q_e (g/g)	26.35	α (g/g s)	2.762
K_1 (s^{-1})	0.268	K_2 (g/g min)	0.0987	β (g/g)	13.403
R^2	0.915	R^2	0.997	R^2	0.947
X^2	2.850	X^2	0.132	X^2	5.823

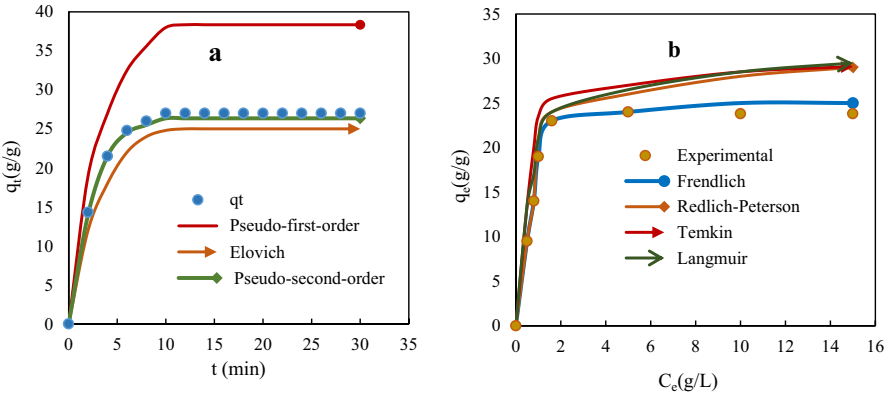

Fig. 10 Sorption kinetic (**a**) and isotherm models (**b**) of the oil sorption onto graft co-polymer at 25 mL oil/1.0 L seawater system, 100 rpm, and 40 °C

$$\text{The Elovich kinetic model:} \quad dq_t/d_t = \alpha e^{-\beta qt} \tag{9}$$

where q_t and q_e denote the OCS (g/g) at time t and equilibrium, respectively. K_1 (s^{-1}) and K_2 (g/g·min) are the rate constants of pseudo-first-order and pseudo-second-order kinetic models, respectively. The coefficient α (g/g s) is the initial sorption rate, and β (g/g) is the absorption constant.

The sorption kinetic consideration for the co-polymer WHF-g-BA is outlined in Table 6 and Fig. 10a. It should be noted that the sorption kinetic model is appropriate to use with a higher R^2 value and lower X^2 value. As can be seen, the q_e value of 26.35 g/g in the pseudo-second-order model is in agreement with experimental capacity with higher R^2 (0.997) and lower X^2 (0.132) values than the other models. This suggests that the pseudo-second-order kinetic model should be appropriate for the graft co-polymer, and the sorption mechanism involves both physical and chemical processes [16, 36].

Sorption isotherm modelling

As described in the literature [16], isotherm-type models type Langmuir, Freundlich, Temkin, and Redlich-Peterson have been preferentially used to describe the

equilibrium oil uptake on the graft co-polymer WHF-g-BA by nonlinear systems. Figure 10b demonstrates the nonlinear isotherm plots at 40 °C, and the sorption isotherm parameters are listed in Table 7. It is obvious that the Freundlich isotherm achieved the best fitting model with a greater R^2 of 0.986 and lower X^2 of 0.0792 than other isotherms, representing multilayer oil sorption onto the graft co-polymer [37].

Reusability

For both practical and financial reasons, reusability is a crucial consideration when choosing polymeric absorbent materials for oil spill cleanup purposes. Samples are separated using a filter sieve to evaluate their reusability after being absorbed. They are then put in a sand core funnel and left to drain for 10 min in a vacuum medium before being weighed [13–15]. The cycle of sorption and desorption is conducted repeatedly to evaluate the absorbent material's reusability. By pressing 5.0 g of the absorbed oil-extracting fibre from the oil/water system, oil recovery, also known as oil retrieval, is computed.

As shown in Fig. 11, the OCS was higher in the initial cycle and subsequently decreased in the following cycles. In general, the OCS values of the absorbent

Table 7 Results of oil sorption isotherm models at (25 mL oil/1.0 L seawater system, 100 rpm 40 °C)

Models	Nonlinear equations	Parameters	Values
Langmuir	$q_e = \frac{Q_L K_L C_e}{1+K_L C_e}$	C_e = equilibrium oil concentration (g/L)	25.48
		Q_L = constant (g/g)	31.57
		K_L = constant (g/g)	16.04
		R^2	0.942
		X^2	5.163
Freundlich	$q_e = K_F C_e^{1/n}$	K_F = constant (g/g)	21.89
		n = intensity of oil sorption	3.49
		R^2	0.986
		X^2	0.0792
Temkin	$q_e = \frac{RT}{H} Ln(K_T C_e)$	K_T = constant (L/g)	65.865
		H = constant (J/mol)	9.615
		R = universal gas constant (J/mol/K)	8.314
		T = temperature (K)	313
		R^2	0.786
		X^2	13.862
Redlich-Peterson	$q_e = \frac{(K_{RP} C_e)}{(1+A C_e^{\beta})}$	K_{RP} = constant (L/g)	1018.93
		A = constant $(L/g)^{\beta}$	21.875
		β = exponent of adsorption energy	0.735
		R^2	0.941
		X^2	1.268

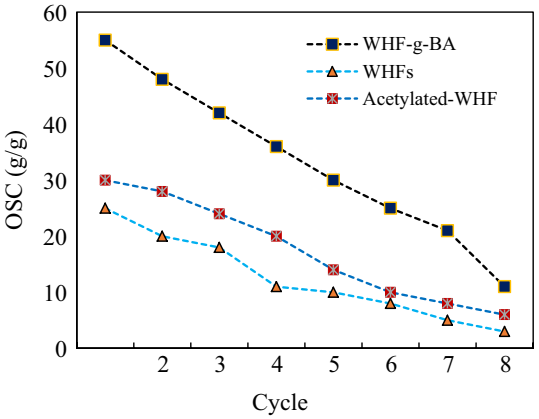

Fig. 11 Sorption-squeezing cycle on the OSC of the WHFs, acetylated-WHF, and WHF-g-BA in the oil/seawater system

material slightly declined from 25.47 to 10.5 g/g for the WHF-g-BA, from 20.16 to 6.5 g/g for the acetylated-WHF, and from 7.46 to 2.5 g/g for the WHFs. This decrease could be the result of a residual oil layer trapped in the material after desorption and the rupture of oil-containing holes under vacuum pressure [38]. The OCS was still at roughly 60% after six cycles. This indicated that the absorbent materials type acetylation, especially graft copolymerisation, can effectively remove oil from the water's surface. This property makes hybrid absorbents perfect materials for a variety of applications, such as effective oil–water separation, removing oil from water in oil spill incidents, and other uses. The enhanced ability of the material derived from the hydrophobic alteration of cellulose fibres to absorb oil offers a means of creating ecologically benign, biodegradable, and reasonably priced oil absorbent materials [39].

Conclusions

Treatment of water hyacinth fibres by acetylation and co-polymerisation approaches increases the hydrophobicity and porous structures. The acetylated product has a porous structure, thus increasing the oil sorption capacity (20.16 g/g) but is lower than the graft co-polymer fibres (25.47 g/g). Through sorption kinetic and isotherm studies, oil sorption to the graft co-polymer has been shown to correlate well with a pseudo-second-order kinetic model and the Freundlich isotherm model. Fibres from water hyacinth and its synthetic materials are economically reused with six cycles of sorption and desorption. Collectively, the graft co-polymers, such as the WHF-g-BA, can be an inexpensive, biodegradable, and rapidly removable alternative sorbent for oil spill cleanup.

Author contributions N.T.T., P.T.T.H., and N.T.D. helped in conceptualization and methodology; N.T.M., L.T.M., and N.D.D. investigated the study; P.N.A. and N.N.L. analysed the data; N.T.S. prepared the manuscript. All authors have read and approved this submission.

Funding No funding.

Declarations

Conflict of interest The authors report no conflicts of interest.

Ethical approval The authors declared that the manuscript is original not published or considered for publications in any other journal.

References

1. Rajabi H, Mosleh MH, Mandal P et al (2020) Emissions of volatile organic compounds from crude oil processing–global emission inventory and environmental release. Sci Total Environ 727:138654. https://doi.org/10.1016/j.scitotenv.2020.138654
2. Habibi Y (2014) Key advances in the chemical modification of nanocelluloses. Chem Soc Rev 43(5):1519–1542. https://doi.org/10.1039/C3CS60204D
3. Wang Y, Yin D, Guo Q, Huang JT (2022) An environmentally friendly method to fabricate superhydrophobic cellulose fiber for oil absorption. Ind Crops Prod 182:114868. https://doi.org/10.1016/j.indcrop.2022.114868
4. Istirokhatun T, Rokhati N, Rachmawaty R, Meriyani M, Priyanto S, Susanto H (2015) Cellulose isolation from tropical water hyacinth for membrane preparation. Procedia Environ Sci 23:274–281. https://doi.org/10.1016/j.proenv.2015.01.041
5. Rakotoarisoa TF, Richter T, Rakotondramanana H, Mantilla-Contreras J (2016) Turning a problem into profit: using Water hyacinth (*Eichhornia crassipes*) for making handicrafts at Lake Alaotra, Madagascar. Econ Bot 70:365–379. https://doi.org/10.1007/s12231-016-9362-y
6. Gaurav GK, Mehmood T, Cheng L, Klemeš JJ, Shrivastava DK (2020) Water hyacinth as a biomass: a review. J Clean Prod 277:122214. https://doi.org/10.1016/j.jclepro.2020.122214
7. Zhang W, Yang P, Cao Y, Yu P, Chen M, Zhou X (2020) Evaluation of fiber surface modification via air plasma on the interfacial behavior of glass fiber reinforced laminated veneer lumber composites. Constr Build Mater 233:117315. https://doi.org/10.1016/j.conbuildmat.2019.117315
8. Sumrith N, Techawinyutham L, Sanjay MR, Dangtungee R, Siengchin S (2020) Characterization of alkaline and silane treated fibers of 'water hyacinth plants' and reinforcement of 'water hyacinth fibers' with bioepoxy to develop fully biobased sustainable ecofriendly composites. J Polym Environ 28:2749–2760. https://doi.org/10.1007/s10924-020-01810-y
9. Tan SJ, Supri AG (2016) Properties of low-density polyethylene/natural rubber/water hyacinth fiber composites: the effect of alkaline treatment. Polym Bull 73:539–557. https://doi.org/10.1007/s00289-015-1508-z
10. Salas-Ruiz A, Mar Barbero-Barrera M, Ruiz-Téllez T (2019) Microstructural and thermo-physical characterization of a Water Hyacinth petiole for thermal insulation particle board manufacture. Materials 12:560. https://doi.org/10.3390/ma12040560
11. Shen X, Xie Y, Wang Q (2017) Improved acetylation efficacy of wood fibers by ionic liquid pretreatment. BioResources 12:684–695. https://doi.org/10.15376/biores.12.1.684-695
12. Teli MD, Terega JM (2021) Solvent-free acetylation of Ensete ventricosum plant fibre to enhance oleophilicity. J Text Inst 113:1958–1966. https://doi.org/10.1080/00405000.2021.1957292
13. Tung NT, Duc NT, Ha PTT et al (2022) A novel rice straw–butyl acrylate graft copolymer: synthesis and adsorption study for oil spill cleanup from seawater. Cellul Chem Technol 56:461–470
14. Tung NT, Duc NT, Ha PTT, Son NT (2022) The graft copolymerization of butyl acrylate and lauryl methacrylate onto sawdust: potential materials for oil spill cleanup. Iran J Sci Technol Trans A Sci 46:385–394. https://doi.org/10.1007/s40995-022-01282-w
15. Tung NT, Duc NT, Ha PTT, Son NT (2021) Oil sorbent based on luffa fiber-graft-poly (butyl acrylate) copolymer. Iran J Sci Technol Trans A Sci 45:1963–1970. https://doi.org/10.1007/s40995-021-01191-4
16. Mahmoud MA (2020) Oil spill cleanup by raw flax fiber: Modification effect, sorption isotherm, kinetics and thermodynamics. Arab J Chem 13:5553–5563. https://doi.org/10.1016/j.arabjc.2020.02.014

17. Sun XF, Sun RC, Sun JX (2004) Acetylation of sugarcane bagasse using NBS as a catalyst under mild reaction conditions for the production of oil sorption-active materials. Bioresour Technol 95(3):343–350. https://doi.org/10.1016/j.biortech.2004.02.025
18. Nagarajappa GB, Pandey KK, Shinde AS, Vagdevi HM (2016) N-Bromosuccinimide (NBS)–an efficient catalyst for acetylation of wood. Holzforschung 70:421–427. https://doi.org/10.1515/hf-2015-0088
19. Ding L, Li Y, Jia D, Deng J, Yang W (2011) β-Cyclodextrin-based oil-absorbents: preparation, high oil absorbency and reusability. Carbohydr Polym 83:1990–1996. https://doi.org/10.1016/j.carbpol.2010.11.005
20. Thakur VK, Thakur MK, Gupta RK (2013) Graft copolymers from cellulose: synthesis, characterization and evaluation. Carbohydr Polym 97(1):18–25. https://doi.org/10.1016/j.carbpol.2013.04.069
21. Rani MJ, Murugan M, Subramaniam P, Subramanian E (2014) A study on water hyacinth *Eichhornia crassipes* as oil sorbent. J Appl Nat Sci 6(1):134–138. https://doi.org/10.31018/jans.v6i1.389
22. Jang J, Kim BS (2000) Studies of crosslinked styrene–alkyl acrylate copolymers for oil absorbency application. I. Synthesis and characterization. J Appl Polym Sci 77:903–913. https://doi.org/10.1002/(SICI)1097-4628(20000725)77:4%3c903::AID-APP26%3e3.0.CO;2-E
23. Arivendan A, Jebas Thangiah WJ, Irulappasamy SN, Chrish B (2022) Study on characterization of water hyacinth (*Eichhornia crassipes*) novel natural fiber as reinforcement with epoxy polymer matrix material for lightweight applications. J Ind Text 51(5):8157S-8174S. https://doi.org/10.1177/15280837211067281
24. Abdelraouf J, Abdelhady HM, Abadir M, Sibak HAE (2022) Kinetics of pyrolysis of water hyacinth: a novel empirical approach Egyptian. J Chem 65(12):467–479
25. Dong T, Wang F, Xu G (2014) Theoretical and experimental study on the oil sorption behavior of kapok assemblies. Ind Crops Prod 61:325–330. https://doi.org/10.1016/j.indcrop.2014.07.020
26. Carneiro MT, Barros AZ, Morais AI, Carvalho Melo AL, Bezerra RD, Osajima JA, Silva-Filho EC (2022) Application of water hyacinth biomass (*Eichhornia crassipes*) as an adsorbent for methylene blue dye from aqueous medium: kinetic and isothermal study. Polymers 14:2732. https://doi.org/10.3390/polym14132732
27. Pathania D, Sharma A (2017) Microwave induced graft copolymerization of binary monomers onto luffa cylindrica fiber: removal of congo red. Procedia Eng 200:408–415. https://doi.org/10.1016/j.proeng.2017.07.057
28. Fiore V, Piperopoulos E, Calabrese L (2019) Assessment of Arundo donax fibers for oil spill recovery applications. Fibers 7(9):75. https://doi.org/10.3390/fib7090075
29. Behnood R, Anvaripour B, Fard NJH, Farasati M (2014) Crude oil layer sorption from saline water surface by raw and acetylated sugarcane bagasse. Sci Int (Lahore) 26:1157–1161. https://doi.org/10.1007/s11771-016-3216-8
30. Matsuno A, Kawamoto K (2023) Assessment of dispersed oil sorption in oily wastewater onto hydrophobized/oleophilized autoclaved aerated concrete (AAC) grains. Environments 10:92. https://doi.org/10.3390/environments10060092
31. El Gheriany IA, El Saqa FA, Amer AAER, Hussein M (2020) Oil spill sorption capacity of raw and thermally modified orange peel waste. Alex Eng J 59:925–932. https://doi.org/10.1016/j.aej.2020.03.024
32. Abdelwahab O, Nasr SM, Thabet WM (2017) Palm fibers and modified palm fibers adsorbents for different oils. Alex Eng J 56:749–755. https://doi.org/10.1016/j.aej.2016.11.020
33. Liu F, Ma M, Zang D, Gao Z, Wang C (2014) Fabrication of superhydrophobic/superoleophilic cotton for application in the field of water/oil separation. Carbohydr Polym 103:480–487. https://doi.org/10.1016/j.carbpol.2013.12.022
34. Singh S, Jelinek R (2020) Solar-mediated oil-spill cleanup by a carbon dot-polyurethane sponge. Carbon 160:196–203. https://doi.org/10.1016/j.carbon.2020.01.016
35. Wahi R, Chuah LA, Choong TSY, Ngaini Z, Nourouzi MM (2013) Oil removal from aqueous state by natural fibrous sorbent: An overview. Sep Purif Technol 113:51–63. https://doi.org/10.1016/j.seppur.2013.04.015
36. Piperopoulos E, Calabrese L, Mastronardo E et al (2019) Assessment of sorption kinetics of carbon nanotube-based composite foams for oil recovery application. J Appl Polym Sci 136:47374. https://doi.org/10.1002/app.47374
37. Balarak D, Mostafapour F, Azarpira H, Joghataei A (2017) Langmuir, Freundlich, Temkin and Dubinin–radushkevich isotherms studies of equilibrium sorption of ampicilin unto montmorillonite nanoparticles. J Pharm Res Int 20:1–9. https://doi.org/10.9734/JPRI/2017/38056

38. Radetić MM, Jocić DM, Jovančić PM, Petrović ZL, Thomas HF (2003) Recycled wool-based nonwoven material as an oil sorbent. Environ Sci Technol 37(5):1008–1012. https://doi.org/10.1021/es0201303
39. Bayık GD, Altın A (2017) Production of sorbent from paper industry solid waste for oil spill cleanup. Mar Pollut Bull 125:341–349. https://doi.org/10.1016/j.marpolbul.2017.09.040